

DISCRETE DIFFRACTION OF LIGHT IN OPTICALLY INDUCED BULK AND PLANAR PHOTONIC SUPERLATTICES IN PHOTOREFRACTIVE LITHIUM NIOBATE

A. V. Gusev,¹ A. V. Kanshu,¹ K. V. Shandarova,¹
V. M. Shandarov,¹ E. V. Smirnov,¹ D. Kip,³
C. Rüter,³ Y. Tan,² and F. Chen²

UDC 535:621.372.8

Experimental multielement planar and channel waveguide structures induced by coherent radiation in bulk samples of photorefractive lithium niobate and planar waveguides on their basis including those formed in a projection scheme with scaling of image dimensions are described. The possibility of linear and nonlinear light localization in optically-induced bulk and planar one-dimensional photorefractive photonic superlattices is demonstrated.

INTRODUCTION

One- and two-dimensional systems of coupled optical waveguides give a unique opportunity of studying the interaction of wave packets with linear and nonlinear systems of different types, since results of these interactions can be visualized in optics [1, 2]. In the first experiments in this field, one-dimensional periodic channel gallium–arsenide-based (GaAs) waveguide systems with Kerr's optical nonlinearity were used [1–3]. Their results have confirmed the possibility of control over the light diffraction and nonlinear light localization in the form of discrete spatial solitons in periodic waveguide systems. However, the effects of light beam self-action in GaAs-based waveguide structures are observed at optical power no less than a few hundred watts. One-dimensional periodic photorefractive channel waveguide systems realized more recently in lithium niobate (LiNbO₃) have allowed a number of effects of nonlinear optical self-action to be observed with microwatt light power [4, 5]. The above-indicated channel waveguide systems are one-dimensional in principle. Two-dimensional systems of coupled waveguides change significantly conditions of light field propagation, and effects that have no analogs in one-dimensional periodic structures can be manifested in them. In [6], a holographic technique of forming two-dimensional photonic lattices (PL) in a strontium–barium niobate (SBN) photorefractive crystal was suggested. The subsequent experimental studies have convincingly demonstrated the advantages of the given approach. Along with the SBN crystals, LiNbO₃ doped with some impurities (for example, Fe and Cu ions) is promising for obtaining optically-induced nonlinear waveguide structures [7–9]. The photorefractive optical nonlinearity of LiNbO₃ is caused by the photovoltaic effect, and its nonlinear response can be observed without application of external electric fields, as in the case of SBN. The general advantage of PL optically induced in photorefractive materials is the possibility of their optical reconfiguration impossible for the channel waveguide structures obtained by the methods of photolithography and thermal diffusion.

Complication of the topology of multielement waveguide structures expands the possibilities of realizing optical analogs of effects inherent in nonlinear quasi-periodic and nonperiodic systems [10, 11]. At the same time, this calls for modification of the methods of optical induction of these structures, since the possibilities of the holographic method based on interference of several coherent light beams appear limited. In the present work, the possibilities of

¹Tomsk State University of Control Systems and Radioelectronics, Tomsk, Russia; e-mail: ShandarovVM@svch.rk.tusur.ru; ²Shandong University, Jinan, the People's Republic of China; ³University of Technology, Clausthal-Zellerfeld, Germany. Translated from *Izvestiya Vysshikh Uchebnykh Zavedenii, Fizika*, No. 9, pp. 57–62, September, 2008. Original article submitted May 15, 2008.

projection and holographic schemes of photorefractive PL optically induced in bulk LiNbO₃ samples and in planar waveguides based on them are demonstrated experimentally together with the special features of the linear and nonlinear discrete light diffraction effects in one-dimensional optically-induced quasi-periodic waveguide systems (photonic superlattices (PSL)).

The photorefractive effect enables modulation of the refractive index of the material to be preformed upon exposure to a spatially nonuniform light field. By this method, it is possible to produce waveguide optical structures with a required topology in bulk samples and planar optical waveguides [7, 8, 12]. The standard holographic technology allows only harmonic modulation of the refractive index of the medium to be obtained. Complication of the topology of optically induced SBN waveguide structures is achieved by significant complication of optical interference schemes for more than two light beams [13, 14]. For LiNbO₃, this problem is slightly simplified, since its slow photorefractive response allows multistep processes of subsequent formation of several PL to be used [12]. In the case of forming PL in plane waveguides, periodic and nonperiodic channel waveguide structures can be induced using coherent or incoherent radiation and amplitude transparencies placed on the waveguide surface [15]. Under illumination of the transparency, the diffraction effects are manifested at distances exceeding the thickness of the waveguide layer typically equal to several micrometers. Thus, the topology of channel structures induced in a planar waveguide is determined by the topology of the transparency [15]. The projection method consists in forming an image of the amplitude transparency on a photosensitive surface or in the volume of a medium with an optical system that allows the image sizes to be scaled. This method possesses better flexibility in comparison with the contact and holographic methods. It allows both periodic and nonperiodic waveguide structures to be formed in a photosensitive medium with variable characteristic sizes of structural elements using the same amplitude transparency.

EXPERIMENTAL SAMPLES

In our experiments, one-dimensional PL and PSL were formed in bulk LiNbO₃: Fe and LiNbO₃: Cu samples and in planar LiNbO₃: Ti: Fe and LiNbO₃: Fe: H⁺ waveguides. The bulk LiNbO₃ samples of congruent composition were doped during crystal growth; the Fe concentration for them varied from 0.005 to 0.1 wt.%, and the Cu concentration was 0.02 wt.%. The planar waveguides were formed in nominally pure LiNbO₃ or LiNbO₃: Fe plates of *X*-cut by two ways. The first included diffusion of titanium (Ti) from the film 10–12 nm thick deposited on the surface of the nominally pure LiNbO₃ plate by the method of vacuum evaporation. Diffusion occurred in air at $T = 1000^\circ\text{C}$ for two hours [12, 16]. As a result, a waveguide layer with a thickness of about 2.5 μm was formed on the substrate surface. Under these conditions, the increase in the extraordinary refractive index on the waveguide surface was $\sim 2 \cdot 10^{-3}$. To modify the photorefractive properties of the waveguide region, the substrates were then doped by Fe ions by thermal diffusion from the film having the thickness from 10 to 60 nm at the same temperature for 20–40 h. The Fe diffusion depth exceeded 20 μm , and its concentration in the waveguide with a thickness of $\sim 2.5 \mu\text{m}$ remained virtually unchanged. The waveguides so prepared provided propagation of the single TE-wave mode on the wavelength $\lambda = 532 \text{ nm}$.

The second group of waveguide samples was prepared in LiNbO₃: Fe (0.1 wt.%) plates of *X*-cut by implantation of protons from an ion beam with 500 keV energy and dose of 10^{17} cm^{-2} [15]. After implantation, the samples were annealed in air at $T = 400^\circ\text{C}$ for 30 min to eliminate point defects and color centers formed in the process of ion implantation. For ion-implanted waveguides, the shape of the refractive index profile was close to a step-like one. In many cases, including implantation of protons into LiNbO₃, the waveguide effect was caused by the layer with disturbed crystal structure and reduced refractive index formed at a certain distance from the irradiated surface. The mode structure and optical losses in the LiNbO₃: Fe: H⁺ waveguides were studied with the help of a prisma-coupling element ($\lambda = 633 \text{ nm}$). For these parameters of the proton implantation process, two TE modes were propagated in the waveguide. Losses for the TE₀ mode did not exceed 1 dB/cm, the TE₁ mode was a leaky wave, and its losses were caused by light tunneling from the waveguide to the substrate through a barrier layer and exceeded 20 dB/cm. The TM modes of light propagation along the *Y* axis were not supported in these waveguides.

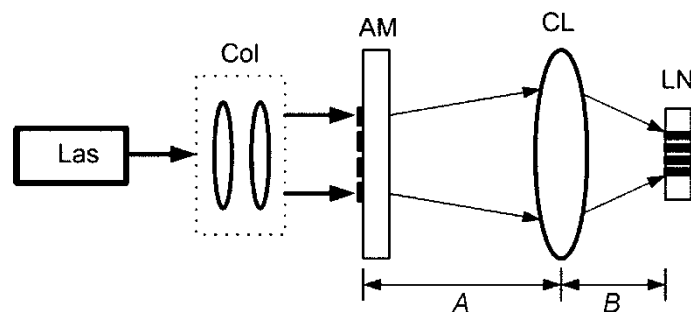


Fig. 1. Scheme of the experiment on projection PL formation in LiNbO_3 samples comprising a laser (Las), a collimator (Col), an amplitude transparency (AM), a cylindrical lens (CL), and a LiNbO_3 sample (LN).

PROJECTION SCHEME OF PL FORMATION

Holographic two-beam [7], contact [15], and projection technologies were used to form PL and PSL in bulk samples and planar waveguides in our experiments. Figure 1 shows the scheme of our experiment for projection PL formation. An LCS-DTL-317 cw solid-state laser (Las) with frequency doubling ($\lambda = 532$ nm with output radiation power of 50 mW) was used as a light source. A collimator (Col) was used to expand the laser beam diameter to ~ 3 cm (at half intensity maximum) for uniform illumination of structures of an amplitude transparency (AM). The structures represent groups of opaque parallel strips (of chromium films) on the standard substrate surface of a 10×10 cm photomask obtained by photolithography. The number of elements in these structures changed from 3 to 50, the strip width and spacing were changed from 20 to 40 μm , and the element length was 18 mm. The image of the structure was projected onto the surface of the LiNbO_3 : Fe (LN) sample with the help of a cylindrical lens (CL) with required scaling coefficient which was varied by changing the distance (A) between the lens (CL) and the transparency plane. The cylindrical lens allowed the image of the transparency to be scaled in the direction of the diffraction structure vector, remaining it unchanged in the direction of elements. The quality of the structure image on the sample surface was controlled with the help of an additional imaging lens, placed behind the sample, and a videocamera. The sample exposure time in different experiments increased from 5 to 60 min for light power of 50 mW. The wave vectors of the formed PL were directed along the optical axis of a crystal.

LINEAR DISCRETE DIFFRACTION OF LIGHT IN ONE-DIMENSIONAL PL AND PSL

Waveguide structures formed on the surface or in the volume of LiNbO_3 samples were investigated by their probing by light beams (He-Ne laser radiation, $\lambda = 633$ nm) in directions normal and parallel to the surface being exposed. For planar PL and PSL, optical probing in the direction normal to the surface provided information on optically induced changes of the refractive index and their characteristics as planar diffraction elements. Excitation of light in such structures along channel waveguide elements or at a certain angle to this direction allowed us to estimate the interelement coupling from discrete light diffraction patterns and to reveal the special features of discrete light diffraction for structures having different topologies. In our experiments, diffraction patterns were investigated by imaging of the exit PL (PSL) plane on the sensor matrix of a videocamera.

Images of light fields in the exit plane of the LiNbO_3 : Fe: Ti optical waveguide (Fig. 2) illustrate the dependence of the discrete light diffraction characteristics on the conditions of optical PL formation. The image in Fig. 2a corresponds to the end-face scheme of light excitation in the initial planar waveguide by a focused beam with a diameter of ~ 5 μm and extraordinary polarization state. The image in Fig. 2b shows the pattern of the beam discrete diffraction in the PL with a spatial period of 10 μm formed using the contact scheme with the amplitude transparency

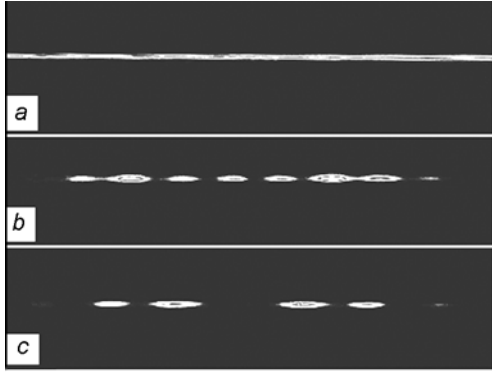


Fig. 2

Fig. 2. Light field patterns in the exit plane of the planar waveguide before (a) and after PL formation (b and c) upon exposure to light through a mask (b) and by the holographic method (c).

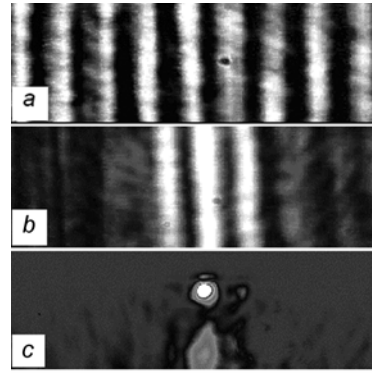


Fig. 3

Fig. 3. Light field patterns in the exit plane of the substrate upon light PL excitation in the bulk sample (a and b) and proton-implanted planar waveguide (c).

illuminated by incoherent UV radiation (the light intensity was $\sim 5 \text{ W/cm}^2$ and the exposure time was 30 s). The image in Fig. 2c corresponds to the pattern of discrete diffraction on PL with a period of $13 \mu\text{m}$ formed by the holographic method using radiation with $\lambda = 532 \text{ nm}$ (the light intensity was $\sim 50 \text{ mW/cm}^2$ and the exposure time was 40 min). In this case, the diffraction patterns differed mainly due to the different PL periods.

Images shown in Fig. 3 illustrate the possibilities of the projective method of PL formation in bulk samples and planar waveguides from LiNbO_3 . The proton-implanted planar $\text{LiNbO}_3: \text{Fe}: \text{H}^+$ waveguide was exposed to light. The waveguide system was formed by imaging of the multielement amplitude transparency structure onto the surface of the X-cut sample. The PL period was $20 \mu\text{m}$ for a $40\text{-}\mu\text{m}$ period of the transparency structure. The sample was exposed for 30 (Fig. 3a and b) and 40 min (Fig. 3c). The patterns shown in Fig. 3a and b were recorded for the PL excited in the substrate volume by parallel (a) and focused light beams (b). The pattern shown in Fig. 3c corresponds to excitation of one PL element induced in the planar waveguide. In this case, tunnel coupling between the neighboring PL elements was weak; therefore, light was trapped in the excited element. At the same time, light was slightly tunneled to the quasi-planar waveguide in the substrate (at the bottom of the image).

To form PSL in bulk samples or planar waveguides, basic one-dimensional PL with the period $\Delta_b = 8\text{--}18 \mu\text{m}$ and changes of the extraordinary refractive index Δn_e from $3 \cdot 10^{-5}$ to 10^{-4} were formed by using the two-beam holographic recording scheme. Then the parameters of the basic structure were modulated with the period $\Lambda_m = 24\text{--}60 \mu\text{m}$ by the holographic method as well. The wave vectors of basic and modulating PL were oriented along the optical axis of LiNbO_3 crystal; the ratio Λ_m/Δ_b varied from 3: 1 to 5: 1. The PL were formed and the channel waveguide structure parameters were modulated by light with $\lambda = 532 \text{ nm}$. The light intensity was in the range from 20 to 100 mW/cm^2 , and the exposure time ranged from 3 to 30 min.

Information on the spatial light field evolution in PL and PSL can be obtained from the light intensity distribution in the exit plane under single-element excitation. In our experiments, these distributions were studied with the help of a videocamera. Images shown in Fig. 4 show light field patterns in the exit planes of the one-dimensional PSL induced in the $\text{LiNbO}_3: \text{Fe}$ sample volume (Fig. 4a–c) and in the planar $\text{LiNbO}_3: \text{Fe}: \text{Ti}$ waveguide (Fig. 4d–f). The patterns shown in Fig. 4a and d illustrate discrete light diffraction in the basic PL with periods of 12 and $13 \mu\text{m}$, respectively. The patterns shown in Fig. 4b, c, e, and f show discrete light diffraction in PSL based on these basic structures with $\Lambda_m/\Delta_b = 3: 1$ upon light excitation of different elements. A focused light beam with a diameter of $\sim 10 \mu\text{m}$, $\lambda = 532 \text{ nm}$, and power of about $1 \mu\text{W}$ was used, which excluded manifestation of light self-action effects during measurements. For the basic PL, the light field patterns were symmetric about the excited waveguide element

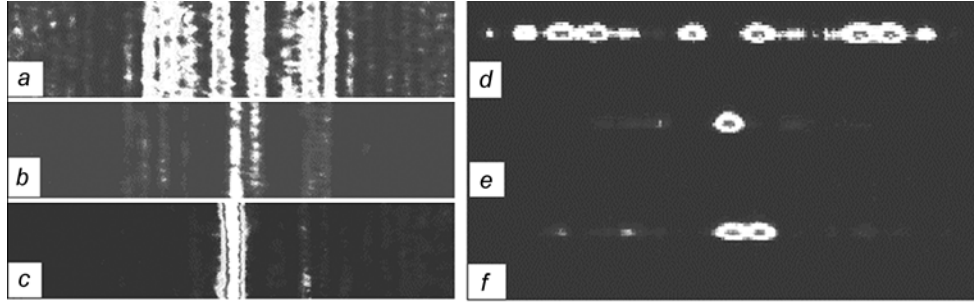


Fig. 4. Light field pattern in the exit PSL plane in the bulk $\text{LiNbO}_3\text{:Fe}$ sample and planar $\text{LiNbO}_3\text{:Fe:Ti}$ waveguide upon single-element excitation in basic PL (*a* and *d*) and PSL regions (*b*, *c*, *e* and *f*).

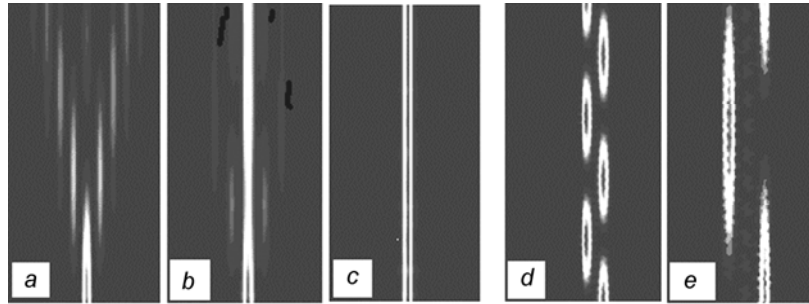


Fig. 5. Results of numerical modeling of light field evolution in the process of light propagation in PSL with $\Lambda_m/\Lambda_b = 3$ (*a-c*) and 4 (*d* and *e*).

(Fig. 4*a* and *d*), in good agreement with [1, 2]. However, the patterns of discrete light diffraction in PSL differed sharply for PSL excitation in different elements of the structure (Fig. 4*b*, *c*, *e*, and *f*). In this case, a strong asymmetry of light intensity distributions and even a complete suppression of the discrete diffraction effect were observed in the linear regime (Fig. 4*c*, *e*, and *f*). Analogous special features were also observed for optically induced PSL with other ratios of modulating and basic waveguide structure spatial periods.

The observed asymmetry of the discrete diffraction patterns and the localization of light energy in the linear regime under excitation of some waveguide elements are explained by a dependence of the PSL waveguide element parameters on their position in the structure. Hence it follows that the propagation constants of waveguide modes in these elements also differ. As a result, the efficiency of light power tunneling to the neighboring waveguide elements can sharply decrease, which causes the probability of linear light localization in the PSL to increase. Optical analogs of Anderson's localization [17] can be observed in cross sections of these structures for the stochastically modulated PL parameters, which also attract attention of the researchers to the optically modulated waveguide structures.

The possibility of linear light localization in the one-dimensional PSL is confirmed by the results of computer modeling of light field evolution in the process of light propagation in PSL with $\Lambda_b = 12 \mu\text{m}$, $\Lambda_m/\Lambda_b = 3$, and a modulation depth of the basic PL of 0.01 (Fig. 5*a*), 0.1 (Fig. 5*b*), and 0.5 (Fig. 5*c*) under single-element excitation. In this case, light was excited in the PSL element with maximal change of the refractive index. For modeling, the beam propagation method was used. It can be seen that already for a basic PL modulation depth of 10% in the linear mode, the effect of discrete diffraction was significantly suppressed in the PL. The patterns shown in Fig. 5*d* and *e* correspond to the light intensity distributions in the PSL with $\Lambda_m/\Lambda_b = 4$ and modulation depth of 50% under light excitation of some of its elements. In this case, the light power can be localized in one or groups of two or three PSL waveguide elements for fixed phase relations between the functions of refractive index profiles of the basic and modulating PL.

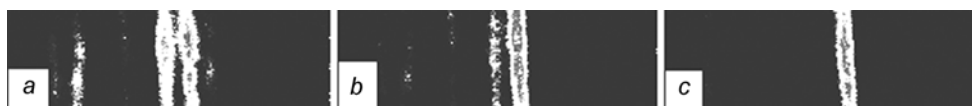


Fig. 6. Light field patterns in the exit PSL plane of the bulk $\text{LiNbO}_3\text{:Fe}$ sample for the nonlinear light localization in one of the elements at $t = 0$ (a), 8 (b), and 31 min (c).

NONLINEAR LIGHT LOCALIZATION IN THE PSL

Nonlinear light propagation in the bulk and planar PSL was studied in the single-element excitation regime for extraordinary light polarization and light power from 1 to 10 μW . Our experiments demonstrated that, as in the case of linear discrete diffraction, the character of light field self-action also significantly depended on the serial number of the excited element. Thus, under excitation of some elements, the light field self-defocusing was observed at which the number of illuminated elements in the exit PSL plane significantly increased with the total light power remaining unchanged. Under excitation of other elements, the quasi-stationary nonlinear light localization in one of the waveguides or nonstationary power transfer between the waveguide elements divided by more than one intermediate waveguide was observed. As an example, Fig. 6 shows the regime of nonlinear light localization in one of the PSL waveguide layers in the $\text{LiNbO}_3\text{:Fe}$ crystal volume. The light beam power in this case was 5 μW , $\lambda = 633$ nm, $\Lambda_b = 13$ μm , $\Lambda_m/\Lambda_b = 3$, and the extraordinary refractive index in the region of basic PL changed by $\Delta n_e = 7 \cdot 10^{-5}$. Just after the light excitation in the PSL ($t = 0$), the main portion of light power ($\sim 80\%$) was localized in two waveguide layers in the exit plane (Fig. 6a). Its concentration in one of these elements was observed with time (Fig. 6 for $t = 8$ min). Time of establishing the quasi-stationary state of nonlinear light localization was 8–10 min. Then the light intensity distribution in the exit PSL plane remained virtually unchanged for more than 30 min.

This work was supported in part by the Russian Foundation for Basic Research (grant 02-39017-GFEN_a) and Chinese National Foundation for Natural Sciences (grants 10505013 and 10711120169).

REFERENCES

1. D. Christodoulides, F. Lederer, and Y. Silberberg, *Nature*, **424**, 817–823 (2003).
2. J. W. Fleischer, G. Bartal, O. Cohen, *et al.*, *Opt. Expr.*, **13**, 1780–1796 (2005).
3. H. S. Eisenberg, Y. Silberberg, Y. Morandotti, *et al.*, *Phys. Rev. Lett.*, **81**, 3383–3386 (1998).
4. F. Chen, M. Stepić, C. Rüter, *et al.*, *Opt. Expr.*, **13**, 4314–4324 (2005).
5. M. Matuszewski, C. R. Rosberg, D. N. Neshev, *et al.*, *Opt. Expr.*, **14**, 254–259 (2006).
6. N. K. Efremidis, S. Sears, D. N. Christodoulides, *et al.*, *Phys. Rev.*, **E66**, 046602 (2002).
7. V. M. Shandarov, K. V. Shandarova, and D. Kip, *Pis'ma Zh. Tekh. Fiz.*, **31**, 88–94 (2005).
8. T. Song, S. M. Liu, R. Guo, *et al.*, *Opt. Expr.*, **14**, 1924–1932 (2006).
9. P. Zhang, D. Yang, J. Zhao, and M. Wang, *Opt. Eng.*, **45**, 074603 (2006).
10. C. R. Rosberg, I. L. Garanovich, A. A. Sukhorukov, *et al.*, *Opt. Lett.*, **31**, 1498–1500 (2006).
11. B. Freedman, G. Bartal, M. Segev, *et al.*, *Nature*, **440**, 1166–1169 (2006).
12. E. Smirnov, C. E. Rüter, D. Kip, *et al.*, *Appl. Phys.*, **B88**, No. 3, 359–362 (2007).
13. C. R. Rosberg, D. N. Neshev, A. A. Sukhorukov, *et al.*, *Opt. Lett.*, **32**, 397–399 (2007).
14. H. Trompeter, W. Krolikowski, D. N. Neshev, *et al.*, *Phys. Rev. Lett.*, **96**, 053903 (2006).
15. Y. Tan, F. Chen, X.-L. Wang, *et al.*, *J. Phys.*, **D41**, 102001 (2008).
16. E. Smirnov, M. Stepić, C. E. Rüter, *et al.*, *Phys. Rev.*, **E74**, 065601(R) (2006).
17. T. Schwartz, G. Bartal, S. Fishman, and M. Segev, *Nature*, **446**, 52–55 (2007).